Microelectronic Engineering 150 (2016) 64–70

Contents lists available at ScienceDirect

Microelectronic Engineering

journal homepage: www.elsevier.com/locate/mee

Scaling approach toward nano electro-discharge machining: Nanoscale patterning of carbon nanotube forests

Zhiming Xiao [a,b,*], Masoud Dahmardeh [a], Mehran Vahdani Moghaddam [a], Alireza Nojeh [a], Kenichi Takahata [a,**]

[a] Department of Electrical and Computer Engineering, University of British Columbia, Vancouver, BC V6T 1Z4, Canada
[b] School of Material and Energy, Guangdong University of Technology, Guangzhou 510006, China

ARTICLE INFO

Article history:
Received 27 July 2015
Received in revised form 25 October 2015
Accepted 12 November 2015
Available online 14 November 2015

Keywords:
Nano patterning
Nano electro-discharge machining
Scaling effect
Breakdown voltage
Carbon nanotube forest

ABSTRACT

Micro-electro-discharge machining (μEDM) is a versatile technique for micromachining of electrically conductive materials with resolutions limited within the micrometer scale. This paper reports an approach to pushing the resolution limit of μEDM down to the nanometer scale. EDM with different electrode tip sizes is performed on carbon nanotube forests and the results reveal a favorable scaling effect of the tip size on the working voltage required for the breakdown of the dielectric between the electrode and workpiece, suggesting that downsizing of the electrode tip assists in the reduction of the discharge pulse energy. Based on this finding, controlled patterning of grating-like structures with ~200 nm height is demonstrated on carbon nanotube forests with an estimated pulse energy of 1 nJ, achieved using a tungsten electrode with a tip radius of 3 μm. Theoretical analysis of this process setting shows a close match with the experimental results, further supporting the scaling effect. These results suggest the feasibility of the approach toward "*nano*-EDM" for an extensive range of potential applications in micro/nanodevice and nanotechnology areas.

1. Introduction

Micromachining has established an essential position in modern manufacturing of a vast range of products including micro-electro-mechanical system (MEMS). Applications of microstructures/components fabricated by micromachining are widespread in broad market segments, e.g., automotive, biomedical, healthcare, electronics, environmental, aerospace, communications, and consumer products [1–3]. A variety of micromachining techniques have been developed. Micro-electro-discharge machining (μEDM) is one of the techniques that have made a significant and unique contribution to this area. The technique utilizes pulses of thermomechanical impact induced by an extremely miniaturized electrical discharge generated between a micro-scale electrode and a workpiece, selectively removing the material of the workpiece. μEDM is a versatile, powerful micromachining process, as it can be applied to any electrically conductive solid-state material regardless of the material's mechanical properties (e.g., hardness and brittleness). The technique is capable of producing three-dimensional (3D) microstructures, and this ability has been utilized to develop a wide range of applications [4]. For example, the use of the technique enabled the development of a self-propelled micromachine achieved with a micro gear reduction system based on hard steel [5] and micromechanical processing tools using super-hard alloys [6]. It can be used to pattern biocompatible bulk metals such as titanium, surgical-grade stainless steels, and nickel–titanium shape memory alloys, leading to the development of advanced biomedical and implantable microdevices [7,8].

Micropatterning of vertically aligned carbon nanotubes, so called CNT forests, has been demonstrated using a dry μEDM method [9]. CNT forests have been attracting significant attention as they offer unique properties suitable for many applications [10–12]. CNT forests are a promising functional bulk material that could be extensively applied to MEMS and other areas that utilize micromachined structures. For instance, aligned CNTs have been used to produce integrated MEMS devices on a wafer scale [13]. Silicon-CNT composite forests have been developed to construct MEMS devices [14]. Microstructures of CNT forests have also been applied to solar cells [15] and fuel cells [16]. However, the shapes of CNT forests grown by typical chemical vapor deposition (CVD) processes with pre-patterned catalyst [17–19] are primarily limited to two-dimensional-like geometries with a uniform height. Dry μEDM processes have been developed to address this constraint, enabling the formation of free form, 3D microstructures in CVD grown CNT forests [9,20,21]. This μEDM approach has enabled micropatterning of as-grown CNT forests, with dimensions as small as 5 μm [9], in a parallel/batch mode [22]. CNT-forest-based devices have been developed with 3D shaping of the forest performed using this technique [23,24].

It is well known that microstructures larger than 5 μm can be easily created using μEDM [25,26]. Attempts to improve the smallest machinable size have been made to show a miniaturization limit as small as

* Correspondence to: Z. Xiao, Department of Electrical and Computer Engineering, University of British Columbia, Vancouver, BC, V6T 1Z4, Canada.
** Corresponding author.
E-mail addresses: xiaozmpe@gmail.com (Z. Xiao), takahata@ece.ubc.ca (K. Takahata).

http://dx.doi.org/10.1016/j.mee.2015.11.008
0167-9317/

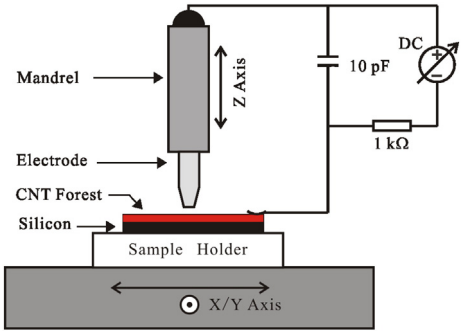

Fig. 1. μEDM set-up used for experiments showing a CNT forest as the workpiece.

1 μm, but not reaching the nano domain so far [27]. The performance of μEDM depends on a number of process parameters. The discharge energy is one of the key parameters. In conventional μEDM (of metals), the energy of a single discharge pulse is on the order of 100 nJ to 10 μJ [28]. Energies down to 1 nJ have been achieved for CNT machining by using a field-emission assisted technique [20]. A high discharge energy causes violent sparks that result in deep craters created by thermal erosion of the workpiece's surface layer, deteriorating surface smoothness and the machining precision. This is one of the factors that limit the removal resolution of μEDM. Pushing the limit of discharge energy is expected to bring nano-scale patterning with μEDM to reality; however, little study has been reported on addressing this challenge.

Here, we report a breakthrough approach based on the scaling effect in μEDM electrodes as a practical and promising means toward realizing the above goal. In particular, downsizing the electrode's tip structures is found to be effective in lowering the working voltage necessary to induce a breakdown of the dielectric between the electrode and workpiece for a given gap size between them, which in turn contributes to ultimate miniaturization of discharge pulse energy and thus maximizing the removal resolution of the process. This very low discharge energy is exploited to demonstrate patterning of arrays of submicron CNT structures, showing the effectiveness of the approach toward "*nano*-EDM". Both experimental and simulation results show that the electrode's tip size and geometry are key factors of the approach. Establishing the ability to 3D pattern CNT-forest structures in the submicron regime and beyond could pave an alternative way to vacuum micro/nano-electronics and field-emission-type devices such as displays, among other applications in the nanotechnology and MEMS fields.

2. Experimental method

The μEDM set-up used for machining of CNT forests is illustrated in Fig. 1. This system has a relaxation type resistor capacitor (*R*-*C*) circuit as a discharge pulse generator [29]. The energy provided by this type of circuit to generate discharge can be theoretically expressed as:

$$E = \tfrac{1}{2}(C + C')V^2 \quad (1)$$

where C is the discrete capacitance intentionally placed in the circuit, C' is the total stray capacitance present and coupled with the circuit, and V is the working voltage. According to Eq. (1), either reducing the capacitance or the voltage is a possible path to reducing the discharge energy. For the former case, it is understandable that C' limits the reduction of E even if C is made zero. As the stray capacitance varies widely in different set-ups and samples, this parameter is inherently not a suitable one for precise control of discharge energy. Furthermore, the discharge energy has a quadratic dependence on the voltage whereas it is merely proportional to the capacitance. Therefore, reducing the voltage is a more effective approach to lowering the discharge energy. However, drastic reduction of the working voltage often leads to machining instability due to the decrease of the gap spacing between the electrode and workpiece, causing frequent occurrences of short circuiting. In a typical μEDM setting, the workpiece is submerged in a dielectric liquid (commonly oil or ultrapure water) to perform the removal process; this ambient assists with the flushing of debris produced during the process. The CNT forest, as the workpiece of μEDM, however, cannot be immersed in a liquid, because the aligned CNTs collapse due to the capillary forces when the wetted forest is dried [9]. Therefore, CNT forests are μEDMed in dry ambient, with an oxygen-mixed inert gas, which enables precise etching of the nanotubes with microscopic tool electrodes by establishing pulses of micro discharge between the electrodes and the forest [9,20,21]. With numerical control of the electrode position relative to the forest, free form 3D patterning of the material is made possible.

In a μEDM process, a breakdown of the machining medium, or a spark, is generated when the electric field in the region between the electrode tip and the workpiece surface exceeds the dielectric strength of the medium. The field strength in the region is determined by the gap size and the applied voltage. For a given gap, a certain level of the voltage needs to be applied to produce an electric filed that overcomes the dielectric strength and induces a spark, and this threshold voltage simultaneously determines the level of the discharge energy (Eq. (1)) and hence the amount of material removed by a spark. In a configuration that a voltage is applied between parallel plates, the electric field established in the gap region is uniform and determined only by the gap size. However, for the point-to-plane configuration relevant to the typical μEDM set-up where a fine-tip electrode faces a planar workpiece, the electric field distribution varies with the size and shape of the electrode tip, in which the field enhancement effect [30] plays an important role. This in turn means that the use of differently sized electrodes should lead to different performance levels in μEDM. Here, we investigate the geometrical effects of the electrode on μEDM performance both experimentally and theoretically.

μEDM experiments using different sizes of the electrode were attempted on CNT forests. The forest samples were grown on heavily

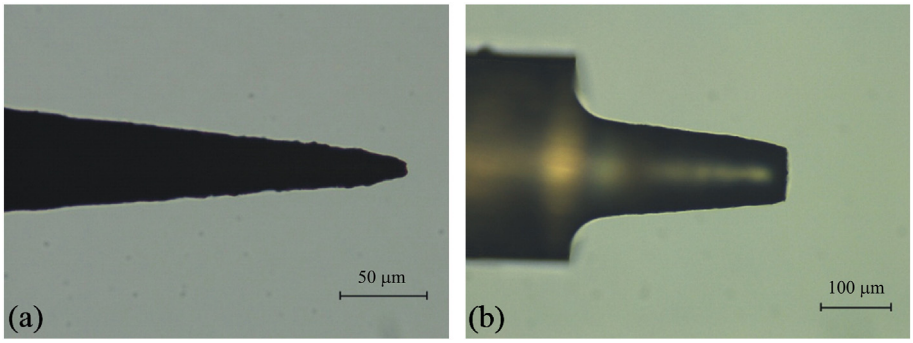

Fig. 2. Optical images of truncated cone electrodes with (a) 3 μm tip radius (Electrode-1), and (b) 37 μm tip radius (Electrode-2).

doped silicon substrate using atmospheric-pressure CVD system. First, the catalyst layer (1 nm thick iron on 10 nm thick alumina) was deposited on a heavily doped silicon wafer using electron beam evaporation. The wafer was then transferred to the reaction tube of the CVD system to synthesize a multi-walled CNT forest with a height of several hundred micrometers using ethylene as the carbon source. Details of the CVD process can be found elsewhere [9,31]. The experiments were performed using a servo-controlled 3-axis μEDM system with 100 nm positioning resolution (EM203, SmalTec International, IL, USA). Two types of electrodes that have truncated cone shapes Electrode-1 and Electrode-2) were prepared by micromachining a pure tungsten wire (with the original diameter of 300 μm) using a technique called wire electro-discharge grinding (WEDG) [32]. The optical images of these two electrodes are shown in Fig. 2. The tip radius of Electrodes-1 and -2 were measured to be approximately 3 μm and 37 μm, respectively. The sidewall slopes of both electrodes were designed to be the same (1/10). For process characterization, these electrodes were scanned over the top surfaces of CNT forests to create square patterns (with a side dimension

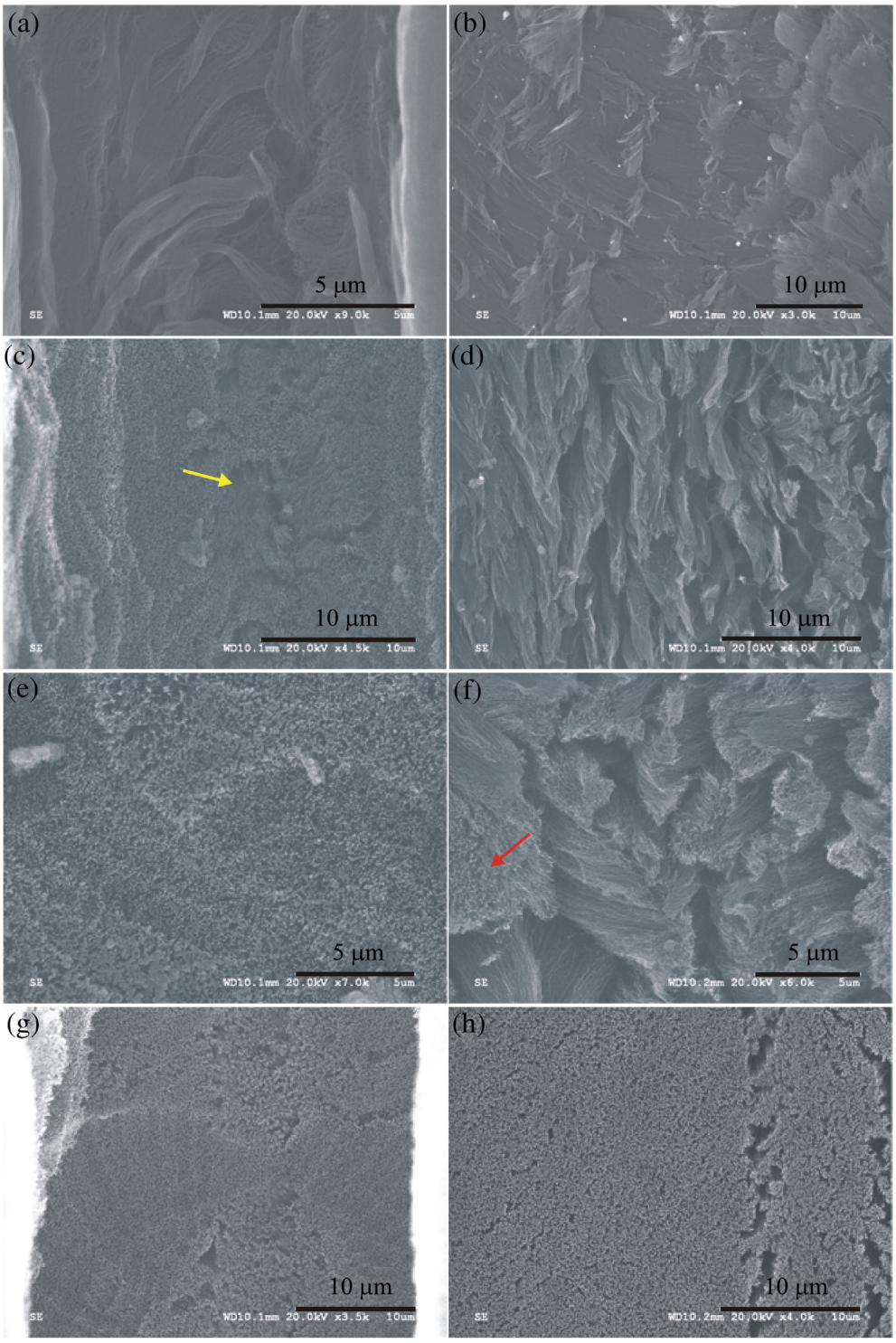

Fig. 3. SEM images of CNT forest surfaces processed using Electrode-1 with estimated discharge energies of (a) 0.25 nJ, (c) 1 nJ, (e) 2.25 nJ, and (g) 4 nJ, and those processed with Electrode-2 with estimated discharge energies of (b) 0.25 nJ, (d) 1 nJ, (f) 2.25 nJ, and (h) 4 nJ.

of 200 μm) using different voltages of 5 V, 10 V, 15 V, and 20 V (corresponding to pulse energies of 0.25 nJ, 1 nJ, 2.25 nJ, and 4 nJ, respectively). These patterns were located adjacent to each other in order to keep all parameters (forest height, density, and surface conditions) as constant as possible, except for the electrode size. The polarity of the voltage was defined so that the CNT forest served as the cathode while the tungsten electrode was the anode (this polarity was reported to yield higher quality in μEDM of CNT forests due to the enhanced field emission properties of CNT forests [20]). The total capacitance of the circuit was ~20 pF (10 pF for C, plus ~10 pF as an approximate value of C' known for the system used). The parasitic capacitance between the electrode tip and the workpiece is estimated to be smaller than the level of C' by 3–5 orders of magnitudes, suggesting that C' is almost the same with the use of either electrode. Both electrodes were rotated at 4000 rpm during all machining tests.

3. Results and discussion

The surfaces of the CNT forests machined using these two electrodes were characterized using a scanning electron microscope (SEM). Fig. 3a, c, e, and g show SEM images of the μEDMed surfaces obtained with Electrode-1, showing the results with different discharge energies corresponding to 0.25 nJ, 1 nJ, 2.25 nJ, and 4 nJ, respectively. Fig. 3b, d, f, and h show the results obtained with Electrode-2 under the same conditions. Fig. 4a is a typical pattern after machining. As can be seen from Fig. 3a and b displaying the cases for the discharge energy of 0.25 nJ (or applied voltage of 5 V), the CNTs were apparently bent laterally showing similar surface morphologies in both cases with Electrodes-1 and -2. Although some discharge pulses were detected during the machining process, the lateral bending suggests that certain mechanical forces acted on the CNTs in the machining process. As a reference, purely mechanical processing, without applying any voltage, under the same electrode rotation/scanning rates was performed on a similar CNT forest. SEM imaging of the mechanically processed surfaces (Fig. 4) indeed shows lateral bending of the CNTs, resulting in a surface morphology similar to the 5 V cases shown in Fig. 3a and b. The above comparison suggests that this particular μEDM condition led to almost purely mechanical processing due to physical contact between the electrode and the CNTs. The results of the 1 nJ (10 V) μEDM with Elecrodes-1 and -2 are displayed in Fig. 3c and d, respectively. It is observable in Fig. 3c that although the machined surfaces contain small portions (shown with an arrow in the figure) that exhibit mechanical bending, most of the regions show high density tips of CNTs, suggesting that the shortening of the CNTs due to the EDM removal partly occurred while preserving the vertical directionality/alignment of the CNTs in those regions and that μEDM played the dominant role in this process with Electrode-1. However, with Electrode-2, mechanical machining was still the main mechanism as can be seen from Fig. 3d, showing laterally flattened CNTs, i.e., 10 V of applied voltage was not large enough to enable EDM removal of the material with the larger electrode. When the discharge energy was increased to 2.25 nJ (15 V), the entire surface processed with Electrode-1 (Fig. 3e) showed CNT tips with no sign of mechanical bending, indicating that the EDM removal was maintained uniformly. With Electrode-2 (Fig. 3f), however, the effect of mechanical bending was still dominant; although traces of μEDM are noticeable in small parts of the processed surface (as shown with an arrow in Fig. 3f), 15 V is evidently not high enough to perform EDM removal with Electrode-2. As the discharge energy was further increased to 4 nJ (20 V), EDM removal was observed in all the processed surfaces with both Electrodes-1 and -2 (Fig. 3g and h, respectively). This experiment shows that a discharge energy of 1 nJ (10 V) or greater is necessary to perform μEDM with Electrode-1, the 3-μm-tip cone, whereas the threshold level increases to 4 nJ (20 V) for the case of Electrode-2, the 37-μm-tip cone. It should be noted that the threshold levels necessary for EDM removal may vary depending on specific sample/experimental settings used (e.g., nanotube geometries, which can influence their field emission ability, and the contact resistance present between the sample and the discharge circuit) that can affect the breakdown voltage as well as pulse current and energy. However, the above finding clearly demonstrates that minimizing the electrode tip size is effective in lowering the threshold discharge energies/voltages required to perform μEDM and hence achieving higher machining resolution and tolerance — a promising result toward nano-scale removal.

Based on the above characterization results, patterning of CNT forests was tested using Electrode-1 and an applied voltage of 10 V. These tests were aimed at creating ordered microstructures with nanoscale heights on the surface of a CNT forest, by scanning the electrode over the forest surface along the X direction of the system while generating discharge pulses. This patterning was implemented by controlling the Z-position of the electrode with varying depths in this process; the X scan of the electrode was repeated while shifting the scan along the Y direction by a distance of 5 μm after each X scan in order to create a rectangular pattern of the processed area. This machining sequence was to partially overlap (along Y) the created trenches as illustrated in Fig. 5, forming a grating-like pattern with a submicron peak-valley cross section. Fig. 6 shows two typical structures patterned on a CNT forest, illustrating the cases of three different removal depths with 5 μm step. SEM analysis and profile measurement revealed that, as seen in the figure, the optimal condition for the target process was achieved when the removal depth was approximately 8 μm; ether smaller or larger depths led to rougher structures (as in the cases of 3 μm and 13 μm depths in Fig. 6a and c, respectively). Under this condition, ordered arrays of shallow, smooth trenches and resultant protruding line structures were reproducibly created as displayed in Fig. 6b and d. The distance between adjacent protruding lines was measured to be ~5 μm, consistent with the programed Y shift of the electrode scan. Atomic force microscopy (AFM) was used to characterize the surface profiles of the machined

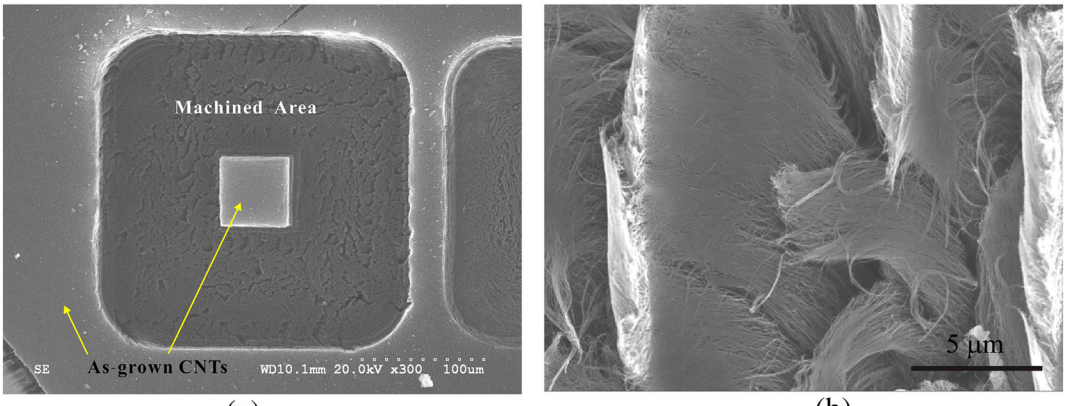

Fig. 4. SEM image of (a) EDM machined pattern, (b) CNT forest surface processed mechanically using a rotating electrode without applying voltage.

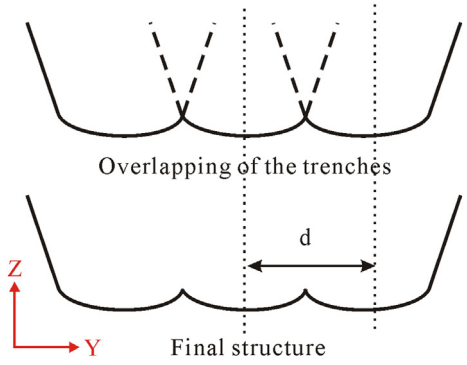

Fig. 5. Illustration of the EDM process for creating grating-like submicron patterns on CNT forest (d = 5 μm).

patterns. AFM imaging (Fig. 7a) and profile data (Fig. 7b) clearly show the morphology of the submicron pattern, verifying that the process created grating-like structures that had triangular cross sections with peak-to-valley heights of ~200 nm or less. These results demonstrate the feasibility of submicron patterning of CNT forests using μEDM, with extremely miniaturized discharge energies with applied voltages down to ~10 V levels.

4. Theoretical analysis: finite element numerical simulation

To further understand the effect of the electrode tip size on μEDM, the finite element method (FEM) was employed to estimate the distribution of electric field between the electrode and workpiece. We used COMSOL Multiphysics® software package (version 3.5) to perform this FEM simulation. The two truncated cone electrodes, Electrodes-1 and -2 described previously were 3D modeled with the tip radius of 3 μm and 37 μm, respectively, to allow direct comparison with the experimental data discussed in the preceding section. The slopes of the sidewalls were also set to be 1/10, the same as in the experiment. Fig. 8a illustrates the two-dimensional (2D) model of the electrodes with a workpiece underneath. The 3D models were formed by rotating the 2D models around their axes. Here, we modeled the workpiece to be a flat sheet of carbon instead of an array of CNTs to simplify the simulation. (There are thousands of CNTs in an area of only several square micrometers, and attempts at modeling all the CNTs explicitly led to an overload of the calculations.) Although there may be small variations in density, orientation, and physical properties of CNTs over the forest material caused by non-uniformity of the catalyst layer and/or variations in the growth process, one can view the material as a relatively uniform bulk, similar to the case of the carbon sheet model. (It should also be noted that the experiments described above with different conditions were analyzed under the same assumption of forest uniformity within small areas.) The distance between the electrode's bottom surface and the surface of the workpiece was set to be 5 μm (a typical discharge gap as observed in the past studies of μEDM of CNT forests [23]). Positive voltages from 5 V to 20 V with a 5 V step were applied to the electrode while the workpiece was grounded. The simulated maps of electric field near the tips of Electrodes-1 and -2 with the same applied voltage of 10 V are shown in Fig. 8b and c, respectively. As can be seen, Electrode-1 with the finer tip created higher field strengths overall, showing the highest being 7.4×10^6 V/m for Electrode-1 at its edges (Fig. 8b), ~3.4× greater than the highest field for Electrode-2 (2.2×10^6 V/m, Fig. 8c); the electric fields near the surface of the carbon sheet were approximately 1.6×10^6 V/m and 2×10^6 V/m, respectively. In the space between two asymmetrical electrodes i.e. the point-to-plane configuration in this study, a breakdown is triggered in the part of the path with highest electric field which exceeds the breakdown strength of the intermediate medium regardless of the field levels in other parts of the path [33]. Under the field, free electrons in the intermediate medium (air in the present case) drift to the positive electrode while producing positive ions (by electron bombardment) and more free electrons, leading to an avalanche phenomenon and breakdown. Fig. 8d shows simulated results of the highest electric field produced

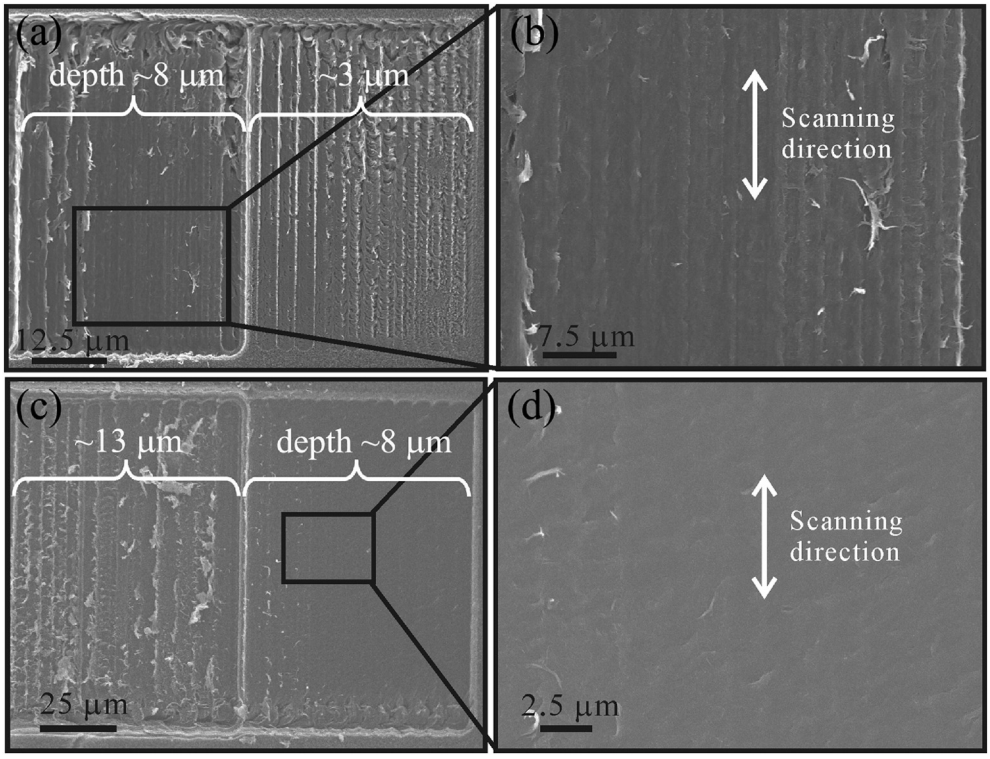

Fig. 6. (a) and (c) show two typical results from submicron EDM patterning on CNT forest with different removal depths. Corresponding close-up images in the regions patterned with a removal depth of ~8 μm are displayed in (b) and (d).

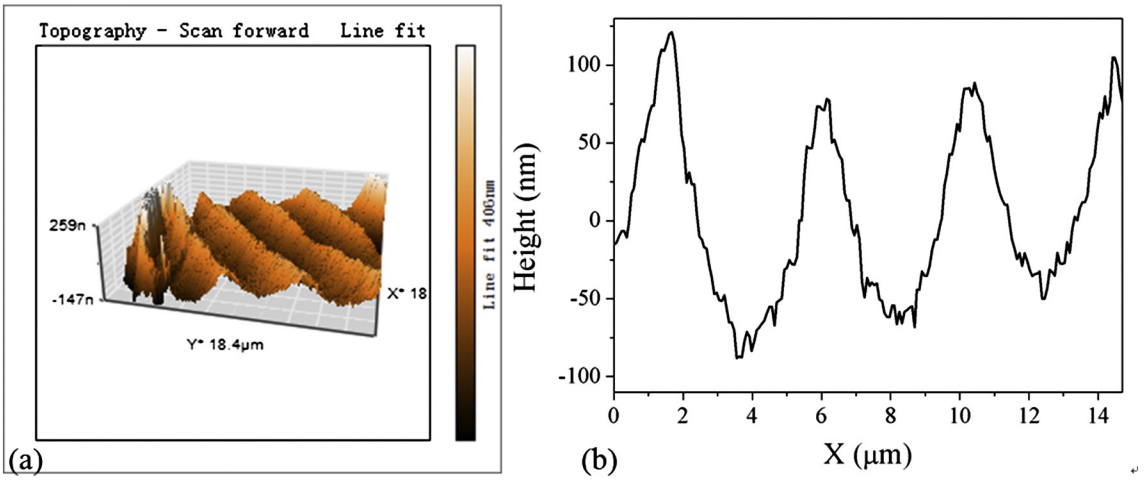

Fig. 7. (a) A 3D morphology of the produced submicron patterns of CNT forest measured with AFM, and (b) cross-sectional profile of the submicron patterns.

with Electrodes-1 and -2 as a function of applied voltage, indicating a clear field enhancement effect from the comparison. The breakdown strength of air was reported to approximately be 3.7–4.5 × 10^6 V/m [34], which is also indicated in Fig. 8d. It can be seen from the graph that the highest electric fields with Electrode-1 for all the voltages used are above the breakdown strength of air (except the 5 V case where the field level is within the threshold region), suggesting that a breakdown will occur with voltages as low as 10 V or perhaps even 5 V. In contrast, the fields with Electrode-2 for 5–15 V are below the threshold, i.e., a breakdown will not be triggered until the voltage increases up to around 20 V. Assuming that a breakdown takes place when the applied voltage causes a field within the breakdown strength range (5 V for Electrode-1 and 20 V for Electrode -2), Fig. 8d suggests that the level of the discharge energy (E) with the former electrode can be 16× smaller than that with the latter electrode for a given applied voltage sufficient to trigger a breakdown. These simulation results, which match well with the experimental results, further demonstrate that the size of the electrode tip has significant effects on the minimum level of breakdown voltage and thus discharge energy in the process.

In a previous study [20] where the CNT forest was set as the cathode the same as in the current study, field enhancement by the CNTs, due to their sharp tips at the top and high aspect ratios, was suggested to assist finer removal in the μEDM process. That implies that the actual electric field at the tips of the CNTs should be higher than the electric field

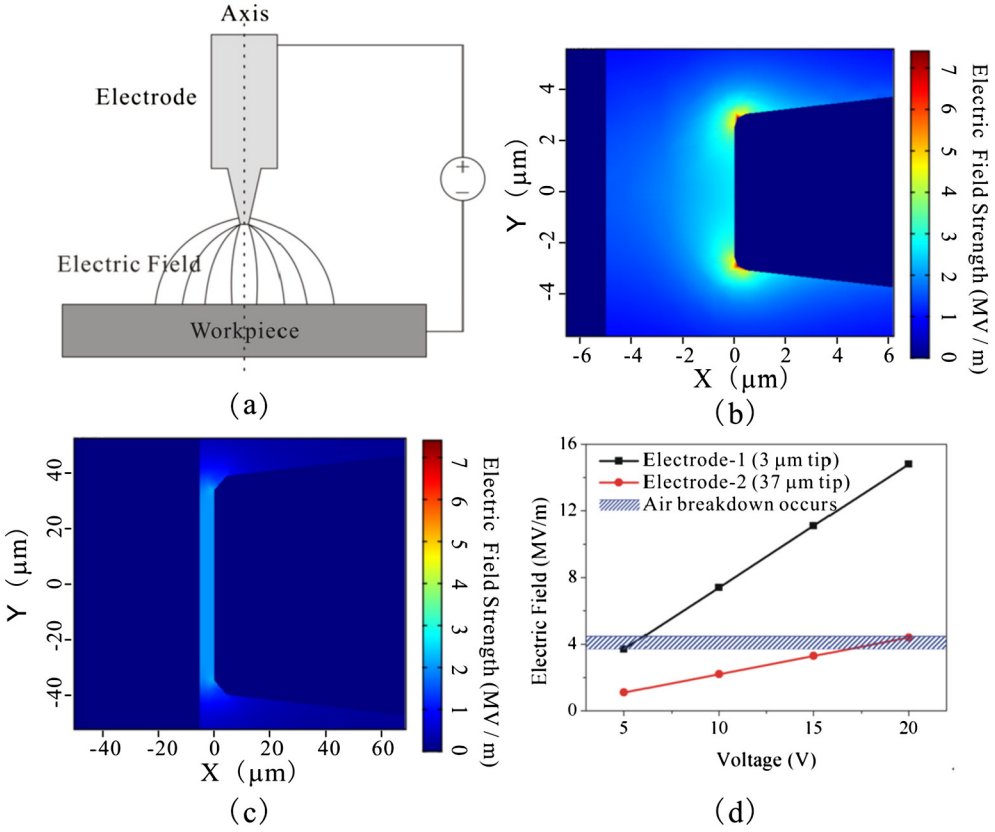

Fig. 8. (a) The 2D model of the electrodes with a workpiece underneath and an electric field established between them. Simulated electric fields near the tips of (b) Electrode-1 and (c) Electrode-2 with the same applied voltage of 10 V. (d) Simulation results of the highest electric field produced with Electrodes-1 and −2 as a function of applied voltage.

obtained from the simulation on the carbon sheet above, which may weaken the decisive effect of the electric field near the electrode tip. Therefore, the question arises as to why in the present study, the strength of the field near the electrode seems to be playing the main role. A possible explanation can be related to the fact that the size of the electrode in the previous work was much larger (~90 μm) than the electrodes in the present case. According to the present simulation results, the field strength at the electrode decreases as the size of the electrode increases. For the case of large electrodes, the field near CNT tips can be stronger than near the electrode. However, as the size of the electrode decreases, the field near the electrode could eventually become stronger than that near the CNT tips. As mentioned before, it was not feasible to simulate the real CNT forest due to computational limitations. However, a simplified simulation was employed to qualitatively explore this possibility; we performed it using a 3D model of a combination of either electrode and an array of 7 × 7 CNTs (diameter and intertube (axis-to-axis) distance of 60 nm and 150 nm, respectively, which are the smallest dimensions our simulations could handle, with a CNT height of 20 μm) that enabled reliable simulation of field distribution at the tips of CNTs. With an applied voltage of 10 V, the peak field on the CNT array was found to be comparable to the field strength on Electrode-2 and 2–2.7× smaller than that on Electrode-1. This result shows the possibility that, even using CNT forests instead of a carbon sheet, the electric field at the electrode may be larger than that at the CNT tips and dominate the breakdown process. However, we note that even this finding may be an artifact of the simulations led by, for example, the effect of mesh size and at what position exactly the maximum field occurs, although we attempted to minimize such effects by using a very fine mesh. Therefore, we cannot definitively conclude that the field near the small electrode is larger than that near CNT tips; however, the close match between the simulation and experimental results support this as a viable option. Regardless of the exact condition involved, we see clearly that the smaller electrode leads to stronger fields for a given applied voltage and thus assists in minimizing the voltage/pulse energy requirements, leading to finer EDM.

5. Conclusion

In conclusion, a μEDM method for extremely miniaturized discharge energy using fine-tipped tungsten electrodes was proposed and studied for submicron patterning of carbon nanotube forests. Experimental testing for dry μEDM of CNT-forest samples in air using electrodes with different tip sizes revealed that the size of the electrode tip affected the breakdown voltage in the dielectric medium of the process and that the reduction of the tip size was an effective path to decreasing the energy of the discharge pulses in the process. The experimental results were supported by simulations. The minimum voltages necessary to conduct EDM removal of the CNTs with these electrodes were measured to match well with theoretically estimated breakdown voltages in air. The use of the electrode with a tip radius of 3 μm was found to enable stable pulse generation with 1 nJ level discharge energies in the process, enabling patterning of grating-like structures with 100 nm order heights on CNT forests. These results show that the machining mechanism based on miniaturized discharge pulses is capable of controlled removal of CNTs in the submicron scale, possibly being extended to even finer patterning through further optimization of process conditions and miniaturization of the electrodes. The outcome also encourages the application of the developed nano-EDM approach to other materials, which could lead to an extensive range of potential applications owing to a very large material base of the EDM process.

Acknowledgments

This work was partially supported by the Natural Sciences and Engineering Research Council of Canada, the Canada Foundation for Innovation, the British Columbia Knowledge Development Fund, and the BCFRST Foundation/British Columbia Innovation Council. K. Takahata is supported by the Canada Research Chairs program. A. Nojeh acknowledges support from the Peter Wall Institute for Advanced Studies.

References

[1] R. Osiander, M. A. G. Darrin, J. L. Champion, CRC Press, 2005 pp 1-12.
[2] K. Santiram, Def. Sci. J. 57 (2007) 209–224.
[3] S. Finkbeiner, Solid-State Device Research Conference (ESSDERC), 2013 9–14.
[4] K. Takahata, IN-TECH, ISBN 978-953-307-027-8, (2009) pp. 143–164.
[5] M. Takeda, K. Namura, K. Nakamura, N. Shibaike, T. Haga, H. Takada, Proc. IEEE Int. Conf. Micro Electro Mech. Syst. 2000 805–810.
[6] K. Takahata, N. Shibaike, H. Guckel, Microsyst. Technol. 6 (2000) 175.
[7] T.A. Fofonoff, S.M. Martel, N.G. Hatsopoulos, J.P. Donoghue, I.W. Hunter, IEEE Trans. Biomed. Eng. 51 (2004) 890–895.
[8] K. Takahata, Y.B. Gianchandani, K.D. Wise, J. Microelectromech. Syst. 15 (2006) 1289–1298.
[9] W. Khalid, M.S.M. Ali, M. Dahmardeh, Y. Choi, P. Yaghoobi, A. Nojeh, K. Takahata, Diam. Relat. Mater. 19 (2010) 1405–1410.
[10] S. Fan, M.G. Chapline, N.R. Franklin, T.W. Tombler, A.M. Cassell, H. Dai, Science 283 (1999) 512–514.
[11] X. Zhang, K. Jiang, C. Feng, P. Liu, L. Zhang, J. Kong, T. Zhang, Q. Li, S. Fan, Adv. Mater. 18 (2006) 1505–1510.
[12] W.H. Wang, T.H. Hong, C.T. Kuo, Carbon 45 (2007) 97–102.
[13] Y. Hayamizu, T. Yamada, K. Mizuno, R.C. Davis, D.N. Futaba, M. Yumura, K. Hata, Nat. Nanotechnol. 3 (2008) 289–294.
[14] D.N. Hutchison, Q. Aten, B. Turner, N. Morrill, L.L. Howell, B.D. Jensen, R.C. Davis, R.R. Vanfleet, Technical Digest of the IEEE International Conference on Solid-State Sensors Actuators, Microsystems (Transducers) Denver CO, 2009 1604–1607.
[15] R.E. Camacho, A.R. Morgan, M.C. Flores, T.A. McLeod, V.S. Kumsomboone, B.J. Mordecai, R. Bhattacharjea, W. Tong, B.K. Wagner, J.D. Flicker, S.P. Turano, W.J. Ready, J. Miner. Met. Mater. Soc. 59 (2007) 39–42.
[16] J. Yang, D.J. Liu, Carbon 45 (2007) 2845–2848.
[17] J.J. Sohn, S. Lee, Y.H. Song, S.Y. Choi, K.J. Cho, K.S. Nam, Appl. Phys. Lett. 78 (2001) 901–903.
[18] K. Hata, D.N. Futaba, K. Mizuno, T. Namai, M. Yumura, S. Iijima, Science 306 (2004) 1362–1364.
[19] A.J. Hart, A.H. Slocum, J. Phys. Chem. B. 110 (2006) 8250–8257.
[20] T. Saleh, M. Dahmardeh, A. Bsoul, A. Nojeh, K. Takahata, J. Appl. Phys. 110 (2011) 103305.
[21] M. Dahmardeh, A. Nojeh, K. Takahata, J. Appl. Phys. 109 (2011) 093308.
[22] M. Sarwar, M. Dahmardeh, T. Saleh, A. Nojeh, K. Takahata, J. Mater. Process. Technol. 214 (2014) 2537–2544.
[23] Z.M. Xiao, M.S. Sarwar, M. Dahmardeh, M. Vahdani Moghaddam, A. Nojeh, K. Takahata, Appl. Phys. Lett. 103 (2013) 171603.
[24] M. Dahmardeh, M. Vahdani Moghaddam, M.H. Tee, A. Nojeh, K. Takahata, Appl. Phys. Lett. 103 (2013) 231606.
[25] F. Han, Y. Yamada, T. Kawakami, M. Kunieda, Precis. Eng. 30 (2006) 123–131.
[26] S. Mahendran, R. Devarajan, T. Nagarajan, A. Majdi, Proceedings of the International Multiconference of Engineers, Computer Scientists Hong Kong, 2010 981–986.
[27] M. Kunieda, Proceedings of the Twenty-third Annual Meeting of the American Society for Precision Engineering, the Twelfth ICPE, 2008 55–60.
[28] S.H. Yeo, G.G. Yap, Int. J. Adv. Manuf. Technol. 18 (2001) 7–11.
[29] M.P. Jahan, Y.S. Wong, M. Rahman, J. Mater. Process. Technol. 209 (2009) 1706–1716.
[30] R.C. Smith, R.D. Forrest, J.D. Carey, W.K. Hsu, Appl. Phys. Lett. 87 (2005) 013111.
[31] M.V. Moghaddam, P. Yaghoobi, A. Nojeh, Appl. Phys. Lett. 101 (2012) 253110.
[32] T. Masuzawa, M. Fujino, K. Kobayashi, T. Suzuki, N. Kinoshita, Ann. CIRP 34 (1985) 431–434.
[33] A. Maglaras, L. Maglaras, Proceedings of the 6th WSEAS International Conference on Applications of Electrical Engineering, 2007 89–95.
[34] C. D. Hodgman, A. Norbert, Chemical Rubber Publishing Co, Cleveland, 1925 pp 547.